Rapid Communications

Tunable space-time crystal in room-temperature magnetodielectrics

Alexander J. E. Kreil,* Halyna Yu. Musiienko-Shmarova, Sebastian Eggert, Alexander A. Serga, and Burkard Hillebrands
Fachbereich Physik and Landesforschungszentrum OPTIMAS, Technische Universität Kaiserslautern, 67663 Kaiserslautern, Germany

Dmytro A. Bozhko
Fachbereich Physik and Landesforschungszentrum OPTIMAS, Technische Universität Kaiserslautern, 67663 Kaiserslautern, Germany and James Watt School of Engineering, University of Glasgow, Glasgow G12 8LT, United Kingdom

Anna Pomyalov and Victor S. L'vov
Department of Chemical and Biological Physics, Weizmann Institute of Science, Rehovot 76100, Israel

(Received 17 November 2018; revised manuscript received 4 March 2019; published 24 July 2019)

We report the experimental realization of a space-time crystal with tunable periodicity in time and space in a magnon Bose-Einstein condensate (BEC), formed in a room-temperature yttrium iron garnet (YIG) film by a microwave space-homogeneous magnetic field. The magnon BEC is prepared to have a well-defined frequency and nonzero wave vector. We demonstrate how the crystalline "density" as well as the time and space textures of the resulting crystal may be tuned by varying the experimental parameters: External static magnetic field, temperature, thickness of the YIG film, and power of the microwave field. The proposed space-time crystals provide an additional dimension for exploring dynamical phases of matter and can serve as a model nonlinear Floquet system, that brings in touch the rich fields of classical nonlinear waves, magnonics, and periodically driven systems.

DOI: 10.1103/PhysRevB.100.020406

Spontaneous symmetry breaking is a fundamental concept of physics. A well-known example is the breaking of spatial translational symmetry, which leads to a phase transition from fluids to solid crystals. By analogy, one can think about a "time crystal" as the result of breaking translational symmetry in time. More generally, one expects the appearance of a "space-time crystal" as a consequence of breaking translational symmetry both in time and in space. If a time crystal exists it should demonstrate time-periodic motion of its ground state [1]. In addition to the time periodicity, the space-time crystals should be periodic in space, similar to an ordinary crystal.

It was recently argued that time crystals and space-time crystals cannot be realized in thermodynamic equilibrium [2,3]. This led to a search for space-time symmetry breaking phenomena in a wider context, for example, in a system with flux equilibrium [4]. Such oscillatory nonequilibrium states are already well known, starting from string and wind musical instruments, such as violins and organs, through quasiperiodic instabilities in plasma and semiconductors (e.g., the Gunn effect [5] used in radar devices) and photon fields in laser resonators, to a microwave generation by nanosized magnetic oscillators driven by a spin-polarized DC electric current [6].

To narrow down a group of candidates to the space-time crystals, that are close to the original idea of the time crystal [1], a set of requirements was proposed [4,7–10]. These include the following: (i) the level of complexity in the interactions merely sufficient to suppress the dissipation of the injected energy in order to ensure very long energy relaxation time relative to other characteristic times of the interaction processes; (ii) requirement on robustness—independence of certain features from the perturbations of the physical system (e.g., the level of disorder); and (iii) spontaneous symmetry breaking, leading to a long-range order and appearance of soft modes of the Nambu-Goldstone type [11].

Possibly the first such example was a periodically driven Floquet quantum system [7], in which the disorder isolates the energy states one from another, suppressing dissipation of the externally pumped energy (see also Refs. [12,13]). Needless to say that none of the previously mentioned examples, such as a violin or the photon field in a laser resonator, meet these criteria.

Natural candidates [14] for time crystals are Bose-Einstein condensates (BECs) in superfluids, trapped cold atoms, and in overpopulated magnon gases [15–19]. Typically, these systems have two characteristic times [15]: The lifetime of the corresponding (quasi)particles τ_N and the energy thermalization time τ_{th} near the bottom of the energy (frequency) spectrum $E_{min} = \hbar\omega_{min}$. If $\tau_{th} \ll \tau_N$, the system first quickly thermalizes toward the local thermodynamic equilibrium with an effective chemical potential μ_{eff} and then slowly relaxes further to the global thermodynamic equilibrium. During the time interval $\tau_{th} \ll \tau \ll \tau_N$ and with a sufficiently large number of (quasi)particles, the system reaches the state with $\mu_{eff} = E_{min}$, creating a BEC, which can be considered as a time crystal with the frequency ω_{min}. Perhaps the most recent observation of a time crystal with very long energy relaxation time is the BEC of magnons in a flexible trap in superfluid ^{3}He-B under periodic driving by an external magnetic field

*kreil@rhrk.uni-kl.de

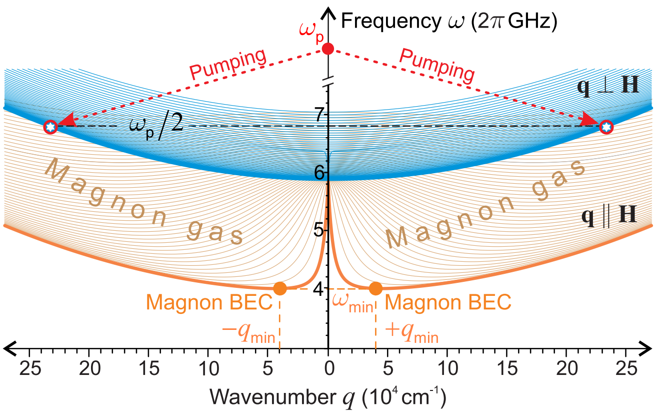

FIG. 1. Magnon spectrum of the first 48 thickness modes in a 5.6-μm-thick YIG film magnetized in plane by a bias magnetic field $H = 1400$ Oe, shown for the wave vector $\boldsymbol{q} \parallel \boldsymbol{H}$ (lower part of the spectrum, orange curves) and for $\boldsymbol{q} \perp \boldsymbol{H}$ (upper part, blue curves). The red arrows illustrate the magnon injection process by means of parallel parametric pumping. Two orange dots indicate the positions of the frequency minimum $\omega_{min}(\pm \boldsymbol{q}_{min})$ occupied by the BECs of magnons.

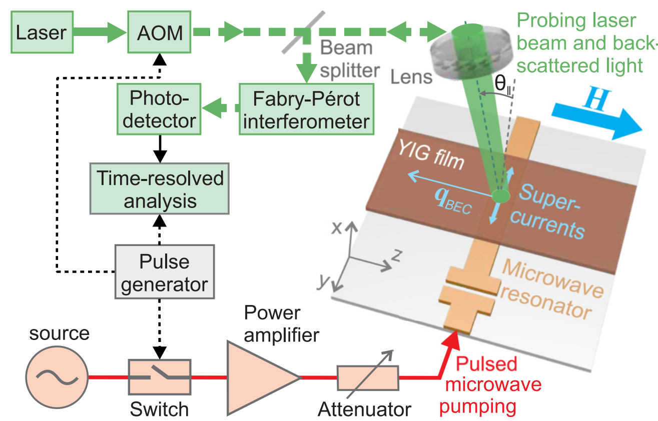

FIG. 2. Experimental setup. The pumping circuit drives a 50-μm-wide microstrip resonator placed below the YIG film by microwave pulses of 2 μs duration with a repetition rate of 1 kHz. Probing light from a solid-state laser ($\lambda = 532$ nm) with a power of 30 mW is chopped by an acousto-optic modulator (AOM) to control the energy input into the YIG sample. The frequency-shifted light, inelastically scattered from magnons, is selected by the tandem Fabry-Pérot interferometer, detected, and analyzed in time.

[14]. The problems related to space-time crystals [20] are more involved and so far were explored mainly theoretically [21–25].

In this Rapid Communication, we report the experimental realization of a space-time crystal (STC) with tunable periodicity in time and space in a magnon BEC formed in a room-temperature yttrium iron garnet (YIG, $Y_3Fe_5O_{12}$) film. The condensate spontaneously arises [17] as a result of scattering of magnons, parametrically pumped by an intense microwave field, to the bottom of their spectrum. We show that this coherent state has the hallmark of nonuniversal relaxation times, which are much longer than the intrinsic timescales and the crystallization time. We consider the interacting magnons, subject to an intensive time-periodic impact, as a model object for studies of Bose-Einstein condensation process in nonlinear Floquet wave systems.

The frequency spectrum of magnons in the in-plane magnetized ferromagnetic YIG film, shown in Fig. 1, has two symmetric minima with nonzero frequency and wave vectors $\omega_{min} = \omega(\pm \boldsymbol{q}_{min})$. The possible BEC has, accordingly, two components with the wave vectors $\pm \boldsymbol{q}_{min}$ and the frequency ω_{min}, creating a standing wave,

$$C(\boldsymbol{r}, t) = C_0 \cos(\boldsymbol{q}_{min} \cdot \boldsymbol{r}) \exp(-i\omega_{min} t). \tag{1}$$

In our experiment (see Fig. 2), we create a BEC by pulsed microwave radiation of frequency $\omega_p = 2\pi \times 13.6$ GHz, which can be considered space homogeneous with a wave number $q_p \approx 0$ [26]. The decay instability of this field with the conservation law,

$$\omega_p \Rightarrow \omega(\boldsymbol{q}) + \omega(-\boldsymbol{q}) = 2\omega(\boldsymbol{q}), \quad \omega(\boldsymbol{q}) = \omega_p/2, \tag{2}$$

excites "parametric" magnons with frequency $\omega(\boldsymbol{q})$ and wave vectors $\pm \boldsymbol{q}$ (see Fig. 1). These parametric magnons further interact mainly via $2 \Leftrightarrow 2$ scattering with the conservation laws,

$$\omega(\boldsymbol{q}_1) + \omega(\boldsymbol{q}_2) = \omega(\boldsymbol{q}_3) + \omega(\boldsymbol{q}_4), \quad \boldsymbol{q}_1 + \boldsymbol{q}_2 = \boldsymbol{q}_3 + \boldsymbol{q}_4, \tag{3}$$

that preserve the total number of magnons and their energy. The theory of weak wave turbulence [27,28] shows that the scattering process (3) leads to a flux of energy towards large $\omega(\boldsymbol{q})$ and to a flux of magnons toward small $\omega(\boldsymbol{q})$, resulting in an accumulation of magnons near the bottom spectrum frequency ω_{min}. The same $2 \Leftrightarrow 2$ processes lead to an efficient thermalization of the bottom magnons during some time $\tau_{th} \lesssim 50$–70 ns and to the subsequent creation of the BEC state [17,29].

The processes leading to the creation of BEC are an experimental manifestation of the STC: A system, driven away from thermodynamic equilibrium by a space-homogeneous, time-periodic (with frequency ω_p) pumping field, spontaneously chooses a space-time periodic state (1) with the frequency ω_{min} and nonzero wave vectors $\pm \boldsymbol{q}_{min}$. Importantly, the parameters ω_{min} and $\pm \boldsymbol{q}_{min}$ are fully determined by intrinsic interactions in the system and are independent of the pumping frequency in a wide range of their values. Note that the lifetime τ_N of the condensate is much longer than τ_{th}, enabling the observation of the magnon BEC state and the study of related effects, such as magnon supercurrents [18] and Nambu-Goldstone modes—the Bogoliubov waves [30]. All these meet the presently accepted requirements of a space-time crystal, listed above.

A more intense pumping process [18,19,31–34] impedes complete condensation of the scattered magnons by mixing their frequencies in the near-bottom zone. The resulting two groups of magnons with a narrow spectral distribution can be considered as *a space-time polycrystal* (STPC) with partial coherence. In this case, the interaction-driven magnon condensation into two coherent spatially extended spin waves—magnon BECs—is completed after the pumping is switched off.

Probing the parametrically pumped magnon gas by means of time-, frequency-, and wave-vector-resolved Brillouin light scattering (BLS) spectroscopy (see Fig. 2) [35–37], we register two density peaks of magnons near the bottom of their spectra ($\omega_{\rm min}$, $\pm\boldsymbol{q}_{\rm min}$). The frequency and wave-vector resolutions of our experimental setup (approximately 100 MHz and 2000 cm^{-1}, respectively) do not allow for the direct detection of the coherence of the magnon BEC [38]. Therefore, we prove the formation of the magnon BEC in a different way, by observation of its physical consequences. In particular, we observe a magnon supercurrent—a macroscopic flow of the magnon condensate induced by a phase gradient imposed on the BEC's wave function [18,39]. In the focal spot heated by the probing laser beam (see Fig. 2), the saturation magnetization $M_{\rm S}$ decreases compared to the rest of the film due to its temperature dependence [40,41], inducing a frequency shift between different parts of the magnon condensate. The resulting phase gradient in the coherent BEC wave function creates a magnon supercurrent, flowing out of the hot spot [18] and leading to a faster decrease of the BLS signal. The detection of such an enhanced decrease allows us to claim the space-time coherence of the observed magnon BEC with a nonzero frequency $\omega_{\rm min}$ and a nonzero wave number $\pm q_{\rm min}$ and to identify it as being a *space-time crystal*.

Now we demonstrate how to control the transition between the STPC and STC magnon phases and how to change all three parameters of the STC described by Eq. (1): The BEC magnon density $|C_0|^2 = N_{\rm BEC}$, the frequency $\omega_{\rm min}$, and the wave number $\pm q_{\rm min}$. Figure 3(a) shows the time evolution of the bottom magnon number $N_{\rm b}(t)$ in the narrow frequency and wave-number intervals determined by the corresponding setup resolutions. The temperature in the light spot was controlled by the duration of the probing laser pulse $\tau_{\rm L}$: The black curve in Fig. 3(a) corresponds to the short duration $\tau_{\rm L} = 6$ μs, when the light spot can be considered as cold; the colored curves correspond to $\tau_{\rm L} = 80$ μs, with a hot light spot.

Comparing the black and red curves in Fig. 3(a), measured at the same pumping power of 31 dBm in the cold and hot laser spots, we see a very similar initial evolution of $N_{\rm b}(t)$ during the action of the pump pulse $t_{\rm p} = -2000$ ns $< t < 0$. At the first stage of this evolution (first 100 ns after switching on of the pumping), $N_{\rm b}(t)$ rapidly grows due to magnon flux toward small $\omega(q)$ as a result of $2 \Leftrightarrow 2$ scattering. For the rest of the pumping time -1900 ns $\lesssim t < 0$, the number of bottom magnons remains unchanged both in the cold and in the hot light spots. This means that the heating-induced magnetic space inhomogeneity practically does not affect the evolution of the bottom magnons in this case. The coherent BEC phase is not created during the pump pulse due to a particular type of $2 \Leftrightarrow 2$ scattering process (3), in which the gaseous bottom magnons with $\omega(\boldsymbol{q}_2) \approx \omega(\boldsymbol{q}_4) \approx \omega_{\rm min}$ scatter on the dense group of parametrically pumped magnons with $\omega(\boldsymbol{q}_1) \approx \omega(\boldsymbol{q}_3) \approx \omega_{\rm p}/2$. This process can be considered as an effective two-magnon ($1 \Leftrightarrow 1$) scattering of the bottom magnons leading to their frequency intermixing (about the frequency linewidth of the parametric magnons). As a result, the frequency spread of the bottom magnon density peak $\Delta\omega$ increases up to $2\pi \times 500$ MHz. Nevertheless, it is still much smaller than $\omega_{\rm min}$, or, keeping analogy to the crystals, the autocorrelation time of these incoherent magnons significantly exceeds their wave period, similarly to the autocorrelation length in polycrystals that spans many unit cell sizes. That is why we consider this magnon state as a *polycrystalline phase* [see the yellow shaded area, marked "Polycrystalline phase-*A*" in Fig. 3(a) for $t < 0$].

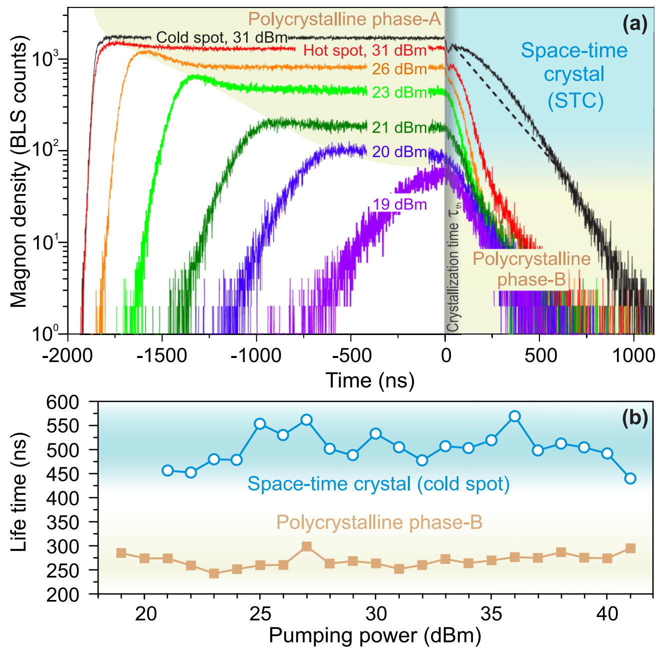

FIG. 3. Transition from the polycrystalline magnon phase to the STC phase and back. (a) Temporal dynamics of the measured magnon density for several pumping power values $P_{\rm pump}$. For $P_{\rm pump} = 31$ dBm two lines are shown measured at different temperatures of the probing spot. The bias magnetic field is $H = 1400$ Oe. (b) The lifetimes of the STC phase, measured in the cold probing spot ($\langle\tau_{\rm LT}\rangle$, circles) and polycrystalline phase-*B* ($\tau_{\rm N}$, squares) as functions of $P_{\rm pump}$. The mean STC lifetimes $\langle\tau_{\rm LT}\rangle$ are determined as the decay times of the exponential curves, connecting the initial and final moments of the existence of the STC phase [see, e.g., the dashed black line in (a)].

After the pump pulse is switched off ($t > 0$ ns), the parametric magnons quickly disappear, preventing further intermixing of the bottom magnons. For a sufficiently strong pumping power ($P_{\rm pump} \gtrsim 20$ dBm), a part of the bottom magnons creates the BEC, the rest of them remain gaseous. The presence of both BEC and noncoherent magnons is confirmed in Fig. 3(a) by a two-stage decay of the bottom magnon density in the hot light spot (red curve, $P_{\rm pump} = 31$ dBm): A fast decay with the mean lifetime $\langle\tau_{\rm LT}\rangle \approx 110$ ns for high $N_{\rm b}(t)$, followed by a much slower decay with $\tau_{\rm N} \approx 250$ ns for $N_{\rm b}(t) < N_{\rm cr} \approx 20$ BLS counts. The faster decay is associated with the existence of the magnon BEC for $N_{\rm b} > N_{\rm cr}$ [see the blue shaded area in Fig. 3(a) labeled "Space-time crystal"]: The magnon supercurrent flowing out of the hot spot enhances the decay rate in the hot spot region [18]. Later, when $N_{\rm b}(t) < N_{\rm cr}$, the magnon BEC and its supercurrent disappear. At this stage, our system returns back to the polycrystalline phase, with an even smaller frequency linewidth $1/\tau_{\rm N} \approx 2\pi \times 0.7$ MHz. This polycrystalline phase-*B* is shown in Fig. 3(a) by a yellow shaded area for $t > 0$.

It is worth noting that the pumping power of 31 dBm used for the measurement of the black top curve in Fig. 3(a) (cold spot) is the same as for the red curve (hot spot), therefore the black curve also corresponds to a well-formed STC at

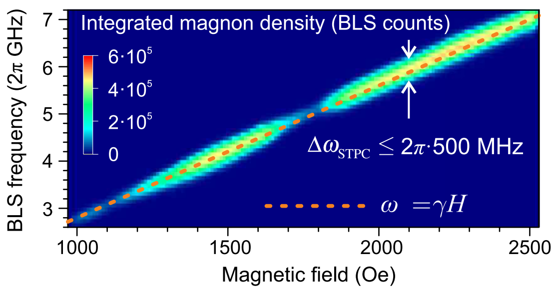

FIG. 4. BLS intensity (color code) and frequency measured during the pump pulse (STPC phase-A) for $q = q_{min}$ as functions of the bias magnetic field H. The BLS intensity reflects the efficiency of the transfer of the parametric magnons to the bottom of the frequency spectrum [34].

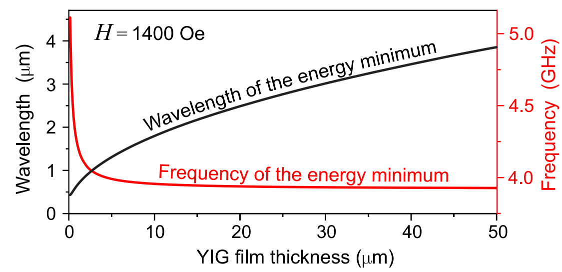

FIG. 5. Theoretical dependencies of the energy minimum wavelength and frequency on the YIG film thickness.

$N_b > N_{cr}$. However, it shows no enhanced decay of the BEC state. The same behavior was observed for all other P_{pump} (not shown). These observations preclude an interpretation of different relaxation rates of the magnon BEC and the incoherent magnon phase in Ref. [43] as being a result of the sensitivity of the BLS technique to the degree of coherence of the scattering magnons. On the other hand, all observed phenomena are well explained by the emergence of a supercurrent that takes away the coherent magnons from the hot spot.

Important information about the STC-STPC phase transition was obtained by tuning the pumping power P_{pump} below 31 dBm. Weaker pumping creates a smaller number of parametrically injected magnons, leading to less effective $2 \Leftrightarrow 2$ magnon scattering and, thus, to an increasing delay in the appearance of these magnons near the bottom of the energy spectrum [Fig. 3(a), lines marked 19–26 dBm]. The resulting density of the bottom magnons decreases as well. Below the threshold density N_{cr}, when the majority of condensed magnons are flown out of the measured region of the BEC, the observed decay rate approaches the same value for all different pumping powers. Importantly, Fig. 3(b) shows that the lifetime of the undisturbed STC in the cold spot is always longer than the lifetime of the corresponding polycrystalline phase. We relate this fact with the continued condensation of gaseous magnons to the BEC phase after the pumping is switched off. These observations clearly prove that the STC density is tunable by the parametric pumping power.

The time periodicity $1/\omega_{min}$ of both the STC and STPC phases can be easily controlled by variation of the bias magnetic field. For example, in the micrometer-thick YIG films, $\omega_{min}(H) \approx \gamma H$, where γ is the gyromagnetic ratio (see Fig. 4).

The spatial periodicity of the STC can be changed in a wide range from 0.5 to 4 μm by a proper choice of the YIG film thickness (see Fig. 5). The magnon condensation was already experimentally demonstrated in micrometer- (see Refs. [17–19,29–32,34,43]) and in nanometer-range-thick YIG films [44,45]. Note that, except for very thin films [44,45], ω_{min} is insensitive to the film thickness.

The tunable magnon space-time crystal and polycrystal, realized in a periodically driven spin system of a room-temperature YIG film, represents an example of a nonlinear Floquet system and therefore serves as a bridge between magnonics and classical nonlinear wave physics from one side and the Floquet time-crystal description of the periodically driven systems from another. Joining these two perspectives may give birth to emergent fields of physical research, "Floquet (or periodically driven) nonlinear wave physics."

The advantage of a macroscopic system that may be studied at room temperature as compared to small samples at millidegrees Kelvin temperatures is obvious. Moreover, broad spectral tunability via the magnitude and direction of the bias magnetic field, strong nonlinearity, nonreciprocity, topology, ability for local manipulations via external electric and magnetic fields, mechanical stress, and sample patterning, being combined with space-, time-, wave-vector-, and frequency-resolved BLS measurements, make the suggested system a good experimental basis for the proposed field. On the other hand, concepts discussed in the framework of the Floquet systems such as quasienergy, umklapp scattering, forbidden bands in quasimomentum space, once applied to magnon space-time crystals, may give insight into the rich physics of this system, creating physical ideas and paving a way to various engineering applications.

Financial support by the European Research Council within the Advanced Grant No. 694709 "SuperMagnonics", by Deutsche Forschungsgemeinschaft (DFG) within the Transregional Collaborative Research Centers SFB/TR49 "Condensed Matter Systems with Variable Many-Body Interaction" (project A7) and SFB/TRR173 "Spin+X – Spin in its collective environment" (project A10) as well as by the DFG Project No. INST 248/178-1 is gratefully acknowledged. D.A.B. acknowledges support from the Alexander von Humboldt Foundation.

[1] F. Wilczek, Quantum Time Crystals, Phys. Rev. Lett. **109**, 160401 (2012).
[2] P. Bruno, Comment on "Quantum Time Crystals", Phys. Rev. Lett. **110**, 118901 (2013).
[3] H. Watanabe and M. Oshikawa, Absence of Quantum Time Crystals, Phys. Rev. Lett. **114**, 251603 (2015).
[4] K. Sacha and J. Zakrzewski, Time crystals: A review, Rep. Prog. Phys. **81**, 016401 (2018).

[5] J. B. Gunn, Instabilities of current in III-V semiconductors, IBM J. Res. Dev. **8**, 141 (1964).

[6] O. R. Sulymenko, O. V. Prokopenko, V. S. Tyberkevych, A. N. Slavin, and A. A. Serga, Bullets and droplets: Two-dimensional spin-wave solitons in modern magnonics, Low Temp. Phys. **44**, 602 (2018).

[7] V. Khemani, A. Lazarides, R. Moessner, and S. L. Sondhi, Phase Structure of Driven Quantum Systems, Phys. Rev. Lett. **116**, 250401 (2016).

[8] C. W. von Keyserlingk, V. Khemani, and S. L. Sondhi, Absolute stability and spatiotemporal long-range order in Floquet systems, Phys. Rev. B **94**, 085112 (2016).

[9] D. V. Else, B. Bauer, and C. Nayak, Floquet Time Crystals, Phys. Rev. Lett. **117**, 090402 (2016).

[10] G. Agarwal, R. E. Allen, I. Bezděková, R. W. Boyd, G. Chen, R. Hanson, D. L. Hawthorne, P. Hemmer, M. B. Kim, O. Kocharovskaya, D. M. Lee, S. K. Lidström, S. Lidström, H. Losert, H. Maier, J. W. Neuberger, M. J. Padgett, M. Raizen, S. Rajendran, E. Rasel *et al.*, Light, the universe and everything—12 Herculean tasks for quantum cowboys and black diamond skiers, J. Mod. Opt. **65**, 1261 (2018).

[11] J. Goldstone, Field theories with "superconductor" solutions, Nuovo Cimento **19**, 154 (1961).

[12] J. Zhang, P. W. Hess, A. Kyprianidis, P. Becker, A. Lee, J. Smith, G. Pagano, I.-D. Potirniche, A. C. Potter, A. Vishwanath, N. Y. Yao, and C. Monroe, Observation of a discrete time crystal, Nature (London) **543**, 217 (2017).

[13] S. Choi, J. Choi, R. Landig, G. Kucsko, H. Zhou, J. Isoya, F. Jelezko, S. Onoda, H. Sumiya, V. Khemani, C. von Keyserlingk, N. Y. Yao, E. Demler, and M. D. Lukin, Observation of discrete time-crystalline order in a disordered dipolar many-body system, Nature (London) **543**, 221 (2017).

[14] S. Autti, V. B. Eltsov, and G. E. Volovik, Observation of a Time Quasicrystal and its Transition to a Superfluid Time Crystal, Phys. Rev. Lett. **120**, 215301 (2018).

[15] G. E. Volovik, On the broken time translation symmetry in macroscopic systems: Precessing states and off-diagonal long-range order, JETP Lett. **98**, 491 (2013).

[16] N. V. Prokof'ev and B. V. Svistunov, Algebraic time crystallization in a two-dimensional superfluid, JETP **154**, 860 (2018).

[17] A. A. Serga, V. S. Tiberkevich, C. W. Sandweg, V. I. Vasyuchka, D. A. Bozhko, A. V. Chumak, T. Neumann, B. Obry, G. A. Melkov, A. N. Slavin, and B. Hillebrands, Bose-Einstein condensation in an ultra-hot gas of pumped magnons, Nat. Commun. **5**, 3452 (2014).

[18] D. A. Bozhko, A. A. Serga, P. Clausen, V. I. Vasyuchka, F. Heussner, G. A. Melkov, A. Pomyalov, V. S. L'vov, and B. Hillebrands, Supercurrent in a room-temperature Bose-Einstein magnon condensate, Nat. Phys. **12**, 1057 (2016).

[19] D. A. Bozhko, P. Clausen, G. A. Melkov, V. S. L'vov, A. Pomyalov, V. I. Vasyuchka, A. V. Chumak, B. Hillebrands, and A. A. Serga, Bottleneck Accumulation of Hybrid Magneto-Elastic Bosons, Phys. Rev. Lett. **118**, 237201 (2017).

[20] J. Smits, L. Liao, H. T. C. Stoof, and P. van der Straten, Observation of a Space-Time Crystal in a Superfluid Quantum Gas, Phys. Rev. Lett. **121**, 185301 (2018).

[21] S. Xu and C. Wu, Space-Time Crystal and Space-Time Group, Phys. Rev. Lett. **120**, 096401 (2018).

[22] G. N. Borzdov, Dirac electron in a chiral space-time crystal created by counterpropagating circularly polarized plane electromagnetic waves, Phys. Rev. A **96**, 042117 (2017).

[23] C. Yannouleas and U. Landman, Trial wave functions for ring-trapped ions and neutral atoms: Microscopic description of the quantum space-time crystal, Phys. Rev. A **96**, 043610 (2017).

[24] T. Li, Z.-X. Gong, Z.-Q. Yin, H. T. Quan, X. Yin, P. Zhang, L.-M. Duan, and X. Zhang, Space-Time Crystals of Trapped Ions, Phys. Rev. Lett. **109**, 163001 (2012).

[25] Z.-L. Deck-Léger and C. Caloz, Scattering in superluminal space-time (ST) modulated electromagnetic crystals, in *Proceedings of the 2017 IEEE International Symposium on Antennas and Propagation & USNC/URSI National Radio Science Meeting* (IEEE, Piscataway, NJ, 2017), pp. 63–64.

[26] V. S. L'vov, *Wave Turbulence Under Parametric Excitation (Applications to Magnets)* (Springer, Berlin, 1994).

[27] V. E. Zakharov, V. S. L'vov, and G. E. Falkovich, *Kolmogorov Spectra of Turbulence I (Wave Turbulence)* (Springer, Berlin, 1992).

[28] Yu. M. Bunkov, E. M. Alakshin, R. R. Gazizulin, A. V. Klochkov, V. V. Kuzmin, V. S. L'vov, and M. S. Tagirov, High-T_c Spin Superfluidity in Antiferromagnets, Phys. Rev. Lett. **108**, 177002 (2012).

[29] P. Clausen, D. A. Bozhko, V. I. Vasyuchka, B. Hillebrands, G. A. Melkov, and A. A. Serga, Stimulated thermalization of a parametrically driven magnon gas as a prerequisite for Bose-Einstein magnon condensation, Phys. Rev. B **91**, 220402(R) (2015).

[30] D. A. Bozhko, A. J. E. Kreil, H. Yu. Musiienko-Shmarova, A. A. Serga, A. Pomyalov, V. S. L'vov, and B. Hillebrands, Bogoliubov waves and distant transport of magnon condensate at room temperature, Nat. Commun. **10**, 2460 (2019).

[31] S. O. Demokritov, V. E. Demidov, O. Dzyapko, G. A. Melkov, A. A. Serga, B. Hillebrands, and A. N. Slavin, Bose-Einstein condensation of quasi-equilibrium magnons at room temperature under pumping, Nature (London) **443**, 430 (2006).

[32] P. Nowik-Boltyk, O. Dzyapko, V. E. Demidov, N. G. Berloff, and S. O. Demokritov, Spatially non-uniform ground state and quantized vortices in a two-component Bose-Einstein condensate of magnons, Sci. Rep. **2**, 482 (2012).

[33] T. Giamarchi, C. Rüegg, and O. Tchernyshyov, Bose-Einstein condensation in magnetic insulators, Nat. Phys. **4**, 198 (2008).

[34] A. J. E. Kreil, D. A. Bozhko, H. Yu. Musiienko-Shmarova, V. S. L'vov, A. Pomyalov, B. Hillebrands, and A. A. Serga, From Kinetic Instability to Bose-Einstein Condensation and Magnon Supercurrents, Phys. Rev. Lett. **121**, 077203 (2018).

[35] C. W. Sandweg, M. B. Jungfleisch, V. I. Vasyuchka, A. A. Serga, P. Clausen, H. Schultheiss, B. Hillebrands, A. Kreisel, and P. Kopietz, Wide-range wavevector selectivity of magnon gases in Brillouin light scattering spectroscopy, Rev. Sci. Instrum. **81**, 073902 (2010).

[36] A. A. Serga, C. W. Sandweg, V. I. Vasyuchka, M. B. Jungfleisch, B. Hillebrands, A. Kreisel, P. Kopietz, and M. P. Kostylev, Brillouin light scattering spectroscopy of parametrically excited dipole-exchange magnons, Phys. Rev. B **86**, 134403 (2012).

[37] O. Büttner, M. Bauer, S. O. Demokritov, B. Hillebrands, Y. S. Kivshar, V. Grimalsky, Y. Rapoport, and A. N. Slavin, Linear and nonlinear diffraction of dipolar spin waves in yttrium iron

garnet films observed by space- and time-resolved Brillouin light scattering, Phys. Rev. B **61**, 11576 (2000).

[38] In Ref. [14] the coherence of a BEC-related time crystal in ^{3}He-B was demonstrated by a direct detection of radio-frequency radiation, caused by the homogeneous precession of the magnetic moment. In YIG films, the typical wave number of the condensed magnons is about $q_{\mathrm{min}} \simeq \pm 10^4$ cm^{-1}, four orders of magnitude larger than the wave number of the electromagnetic field with the same frequency. As a result, the direct microwave radiation by condensed magnons is tremendously suppressed and cannot be detected easily. At the same time, the space periodicity of the magnon BEC formed in parametrically driven YIG films has already been evidenced by means of spatially resolved microfocused BLS spectroscopy [32].

[39] Generally speaking, the observation of the supercurrent is not always sufficient to claim the existence of long-distant space coherence. For example, a similar phenomenon was observed in superfluid ^{3}He-A, demonstrating a tendency to split into many droplets due to the attractive potential. However, in YIG films under the studied conditions, the interaction potential is repulsive [42] and is preventing such an instability.

[40] M. Vogel, A. V. Chumak, E. H. Waller, T. Langner, V. I. Vasyuchka, B. Hillebrands, and G. von Freymann, Optically reconfigurable magnetic materials, Nat. Phys. **11**, 487 (2015).

[41] L. Mihalceanu, V. I. Vasyuchka, D. A. Bozhko, T. Langner, A. Yu. Nechiporuk, V. F. Romanyuk, B. Hillebrands, and A. A. Serga, Temperature-dependent relaxation of dipole-exchange magnons in yttrium iron garnet films, Phys. Rev. B **97**, 214405 (2018).

[42] O. Dzyapko, I. Lisenkov, P. Nowik-Boltyk, V. E. Demidov, S. O. Demokritov, B. Koene, A. Kirilyuk, T. Rasing, V. Tiberkevich, and A. Slavin, Magnon-magnon interactions in a room-temperature magnonic Bose-Einstein condensate, Phys. Rev. B **96**, 064438 (2017).

[43] V. E. Demidov, O. Dzyapko, S. O. Demokritov, G. A. Melkov, and A. N. Slavin, Observation of Spontaneous Coherence in Bose-Einstein Condensate of Magnons, Phys. Rev. Lett. **100**, 047205 (2008).

[44] C. Safranski, I. Barsukov, H. K. Lee, T. Schneider, A. A. Jara, A. Smith, H. Chang, K. Lenz, J. Lindner, Y. Tserkovnyak, M. Wu, and I. N. Krivorotov, Spin caloritronic nanooscillator, Nat. Commun. **8**, 117 (2017).

[45] M. Schneider, T. Brächer, V. Lauer, P. Pirro, D. A. Bozhko, A. A. Serga, H. Yu. Musiienko-Shmarova, B. Heinz, Q. Wang, T. Meyer, F. Heussner, S. Keller, E. Th. Papaioannou, B. Lägel, T. Löber, V. S. Tiberkevich, A. N. Slavin, C. Dubs, B. Hillebrands, and A. V. Chumak, Bose-Einstein condensation of quasi-particles by rapid cooling, arXiv:1612.07305.